# Georg-August-Universität

# Göttingen


## STABILIZED FEM FOR INCOMPRESSIBLE FLOW.

## CRITICAL REVIEW AND NEW TRENDS

**G. Lube**

**Preprint Nr. 2006-14**

Preprint-Serie des
Instituts für Numerische und Angewandte Mathematik
Lotzestr. 16-18
D - 37083 Göttingen

European Conference on Computational Fluid Dynamics
ECCOMAS CFD 2006
P. Wesseling, E. Oñate and J. Périaux (Eds)


# STABILIZED FEM FOR INCOMPRESSIBLE FLOW. CRITICAL REVIEW AND NEW TRENDS

**G. Lube***

*Georg-August University of Göttingen, Math. Department, NAM
Lotzestrasse 16-18, D-37083 Göttingen, Germany
e-mail: lube@math.uni-goettingen.de
web page: http://www.num.math.uni-goettingen.de/lube/

**Key words:** Incompressible flow, Navier-Stokes equations, stabilized finite elements, variational multiscale methods, subgrid viscosity

**Abstract.** *The numerical solution of the nonstationary, incompressible Navier-Stokes model can be split into linearized auxiliary problems of Oseen type. We present in a unique way different stabilization techniques of finite element schemes on isotropic and hybrid meshes. First we describe the state-of-the-art for the classical residual-based SUPG/PSPG method. Then we discuss recent symmetric stabilization techniques which avoid some drawbacks of the classical method. These methods are closely related to the concept of variational multiscale methods which provides a new approach to large eddy simulation.*

## 1 INTRODUCTION

We consider the nonstationary, incompressible Navier-Stokes problem

$$\partial_t \mathbf{u} - \nu \Delta \mathbf{u} + (\mathbf{u} \cdot \nabla)\mathbf{u} + \nabla p = \tilde{\mathbf{f}}, \tag{1}$$

$$\nabla \cdot \mathbf{u} = 0 \tag{2}$$

for velocity $\mathbf{u}$ and pressure $p$ in a polyhedral domain $\Omega \subset \mathbb{R}^d$, $d \leq 3$, with a given source term $\tilde{\mathbf{f}}$. An A-stable low-order time discretization (possibly with time step control) is applied in an outer loop,. In an inner loop, we decouple and linearize the resulting system using a Newton-type iteration per time step. This leads to problems of Oseen type:

$$L_{Os}(\mathbf{b}; \mathbf{u}, p) := -\nu \Delta \mathbf{u} + (\mathbf{b} \cdot \nabla)\mathbf{u} + c\mathbf{u} + \nabla p = \mathbf{f}, \quad \text{in } \Omega, \tag{3}$$

$$\nabla \cdot \mathbf{u} = 0 \quad \text{in } \Omega. \tag{4}$$

Also the iterative solution of the steady state Navier-Stokes equations using a fixed point iteration leads to problems of type (3)-(4) with $c = 0$. Moreover, this approach can be extended to more complex models including thermally coupled and/or turbulent flows, see, e.g., [23, 28].

The basic Galerkin finite element method (FEM) for (3)-(4) may suffer from: (i) dominating advection (and reaction) in the case $0 < \nu \ll 1$, and/or (ii) violation of the discrete inf-sup (or Babuška-Brezzi) stability condition for the velocity and pressure approximations. The *streamline upwind/Petrov-Galerkin (SUPG) method*, introduced in [7], and the *pressure-stabilization/Petrov-Galerkin* (PSPG) method, introduced in [26, 21], allow to treat both problems in a unique framework using rather arbitrary FE approximations of velocity and pressure, including equal-order pairs. Additionally to the Galerkin part, the elementwise residual $L_{Os}(\mathbf{b};\mathbf{u},p)-\mathbf{f}$ is tested against the (weighted) non-symmetric part $(\mathbf{b}\cdot\nabla)\mathbf{v}+\nabla q$ of $L_{Os}(\mathbf{b};\mathbf{v},q)$. It was shown in [14, 18, 31] that an additional element-wise stabilization of the divergence constraint (4), henceforth denoted as *grad-div stabilization*, is important if $0 < \nu \ll 1$. Due to its construction, we classify the SUPG/PSPG/grad-div approach as an *(element-wise) residual-based stabilization* technique.

Despite the striking success of these stabilization techniques to incompressible flows over the last 20 years, there are some drawbacks which are basically due to the strong coupling between velocity and pressure in the stabilizing terms, see e.g. [5, 15, 8]. Several attempts have been made to relax the strong coupling of velocity and pressure and to introduce symmetric versions of the stabilization terms :

The interior penalty technique of the discontinuous Galerkin (DG) method was applied in the framework of continuous approximation spaces leading to the *edge/face oriented stabilization* introduced in [8]. Another approach consists in *projection-based stabilization* techniques. The first step was done in [12] where weighted *global* orthogonal projections of the non-symmetric terms in (3)-(4) are added to the Galerkin scheme. A related *local* projection technique has been applied to the Oseen problem in [4] with low-order equal-order interpolation. Another projection-based stabilization was introduced in [27, 25]. Projection-based methods are closely related to the framework of variational multiscale methods, see [20], which provide a new approach to large eddy simulation (LES).

In this review paper, we present the state-of-the-art of residual-based stabilization techniques and discuss recent projection-based stabilization techniques for the Oseen problem (3)-(4), together with a critical comparison. For brevity, we consider only *conforming* FEM. An extension to a non-conforming approach like DG-methods can be found, e.g., in [10] or [16]. The latter methods are not robust with respect to the viscosity $\nu$. Appropriate stabilization mechanisms for DG-methods are given in [6].

The paper is organized as follows: In Sec. 2, we describe the basic Galerkin discretization of the Oseen problem. Then, we consider the residual-based SUPG/PSPG/grad-div stabilization following [29, 2], see Sec. 3. As a step towards symmetric stabilization techniques, we consider in Sec. 4 reduced stabilized schemes which omit the PSPG stabilization in case of inf-sup stable velocity-pressure approximation. Next, we present symmetric projection-based stabilization techniques. Here, we review the local projection approach proposed in [4] and another projection-based stabilized scheme due to [27, 25], see Sec. 5.

Throughout the paper, we use standard notations for Lebesgue and Sobolev spaces. The $L^2$-inner product in a domain $\omega$ is denoted by $(\cdot,\cdot)_\omega$. We omit the index for $\omega=\Omega$.

## 2 STANDARD GALERKIN FEM FOR THE OSEEN MODEL

This section describes the standard Galerkin FEM for the Oseen-type problem

$$
\begin{aligned}
L_{Os}(\mathbf{b};\mathbf{u},p) := -\nu\Delta\mathbf{u} + (\mathbf{b}\cdot\nabla)\mathbf{u} + c\mathbf{u} + \nabla p &= \mathbf{f} \quad \text{in } \Omega, && (5)\\
\nabla\cdot\mathbf{u} &= 0 \quad \text{in } \Omega, && (6)\\
\mathbf{u} &= \mathbf{0} \quad \text{on } \partial\Omega && (7)
\end{aligned}
$$

with $\mathbf{b}\in[H^1(\Omega)]^d,\ (\nabla\cdot\mathbf{b})(x)=0,\ \mathbf{f}\in[L^2(\Omega)]^d$ and constants $\nu>0,\ c\geq 0$. For brevity, we use homogeneous Dirichlet data.

The variational formulation reads: find $U:=\{\mathbf{u},p\}\in\mathbf{W}:=\mathbf{V}\times\mathbf{Q}:=[H_0^1(\Omega)]^d\times L_0^2(\Omega)$ with $L_0^2(\Omega):=\{q\in L^2(\Omega)\mid \int_\Omega q\,dx=0\}$, s.t.

$$
\mathcal{A}(\mathbf{b};U,V)=\mathcal{L}(V)\qquad \forall\, V=\{\mathbf{v},q\}\in\mathbf{V}\times\mathbf{Q}, \tag{8}
$$

with

$$
\begin{aligned}
\mathcal{A}(\mathbf{b};U,V) &= (\nu\nabla\mathbf{u},\nabla\mathbf{v})_\Omega + ((\mathbf{b}\cdot\nabla)\mathbf{u}+c\mathbf{u},\ \mathbf{v})_\Omega - (p,\ \nabla\cdot\mathbf{v})_\Omega + (q,\ \nabla\cdot\mathbf{u})_\Omega, && (9)\\
\mathcal{L}(V) &= (\mathbf{f},\ \mathbf{v})_\Omega. && (10)
\end{aligned}
$$

Let $\mathcal{T}_h$ be an admissible triangulation of the polygonal/polyhedral domain $\Omega$ where each element $T\in\mathcal{T}_h$ is a smooth bijective image of a unit element $\hat{T}$, i.e., $T=F_T(\hat{T})$ for all $T\in\mathcal{T}_h$. Here, $\hat{T}$ is the unit simplex or the unit hypercube in $\mathbb{R}^d$ or, in the three-dimensional case, the unit triangular prism. A mixture of element types is admitted; in this case we use for each type the appropiate reference element. On this mesh, we consider Lagrangian finite elements of order $r\in\mathbb{N}$, i. e., $\mathcal{P}_r(\hat{T})$ denotes the polynomial space on the reference element that contains the set $\mathcal{P}_r$ of polynomials of degree $r$. We set

$$
X_h^r=\{v\in C(\bar{\Omega})\mid\ v|_T\circ F_T\in\mathcal{P}_r(\hat{T})\ \forall T\in\mathcal{T}_h\} \tag{11}
$$

and introduce conforming finite element spaces for velocity and pressure

$$
\mathbf{V}_h^r\ :=\left[H_0^1(\Omega)\cap X_h^r\right]^d,\quad \mathbf{Q}_h^s\ :=L_0^2(\Omega)\cap X_h^s,\qquad r,s\in\mathbb{N}. \tag{12}
$$

We use continuous pressure in order to avoid integrals on interelement boundaries after partial integration later on. Clearly, other conforming discrete spaces for the velocity and the pressure can be chosen (e.g., enriched with bubble functions). Moreover, for brevity, we will not present possible extensions to non-conforming methods.

The Galerkin method reads: find $U=\{\mathbf{u},p\}\in\mathbf{W}_h^{r,s}:=\mathbf{V}_h^r\times\mathbf{Q}_h^s$, s. t.

$$
\mathcal{A}(\mathbf{b};U,V)=\mathcal{L}(V)\quad\forall\, V=\{\mathbf{v},q\}\in\mathbf{W}_h^{r,s}. \tag{13}
$$

Well-known sources of instabilities of the Galerkin finite element method (13) stem from dominating advection and from the violation of the discrete inf-sup condition

$$
\exists\beta_0>0:\quad \inf_{q_h\in\mathbf{Q}_h^s}\sup_{\mathbf{v}_h\in\mathbf{V}_h^r}\frac{(q_h,\nabla\cdot\mathbf{v}_h)}{\|\nabla\mathbf{v}_h\|_{[L^2(\Omega)]^{d\times d}}\|q_h\|_{L^2(\Omega)}}\geq\beta_0, \tag{14}
$$

where $\beta_0$ can be chosen independent of $h$. Condition (14) is not valid in the case of equal-order velocity-pressure FE spaces $\mathbf{V}_h^r \times \mathbf{Q}_h^r$. Moreover, in case of anisotropic elements, even inf-sup stable FEM are often not robust w.r.t. the maximal aspect ratio of the elements $T$.

## 3 CLASSICAL RESIDUAL-BASED STABILIZATION METHODS

The classical stabilization of the Galerkin scheme (13) is a combination of pressure stabilization (PSPG) and streamline-upwind stabilization for advection (SUPG) together with a stabilization of the divergence constraint: find $U_h = \{\mathbf{u}_h, p_h\} \in \mathbf{W}_h^{r,s}$, s.t.

$$\mathcal{A}_{rbs}(\mathbf{b}; U_h, V_h) = \mathcal{L}_{rbs}(V_h) \quad \forall\, V_h = \{\mathbf{v}_h, q_h\} \in \mathbf{W}_h^{r,s} \tag{15}$$

with

$$\begin{aligned} \mathcal{A}_{rbs}(\mathbf{b}; U, V) \;:=\; & \mathcal{A}(\mathbf{b}; U, V) \;+\; \underbrace{\sum_{T\in\mathcal{T}_h} \gamma_T\, (\nabla\cdot\mathbf{u}, \nabla\cdot\mathbf{v})_T}_{grad-div\ stabilization} \qquad (16)\\ & + \underbrace{\sum_{T\in\mathcal{T}_h} (L_{Os}(\mathbf{b}; \mathbf{u}, p),\ \delta_T^u(\mathbf{b}\cdot\nabla)\mathbf{v} + \delta_T^p \nabla q)_T}_{SUPG+PSPG\ stabilization}, \\ \mathcal{L}_{rbs}(V) \;:=\; & \mathcal{L}(V) \;+\; \overbrace{\sum_{T\in\mathcal{T}_h} (\mathbf{f}, \delta_T^u(\mathbf{b}\cdot\nabla)\mathbf{v} + \delta_T^p\nabla q)_T} \qquad (17) \end{aligned}$$

containing the three parameter sets $\{\delta_T^u\}, \{\delta_T^p\}$ and $\{\gamma_T\}$ depending on the choice of the FE spaces, see below. During this chapter, we focus on the case $\delta_T = \delta_T^u = \delta_T^p$. (For an extension to the case $0 \le \delta_T^p = \delta_T^u$, we refer to Remark 4.2 in Sec. 4.)

The stabilizing effect stems from additional control of the term $\sum_T \gamma_T \|\nabla\cdot\mathbf{u}\|^2_{L^2(T)}$ and of the SUPG/PSPG-term $\sum_T \delta_T \|(\mathbf{b}\cdot\nabla)\mathbf{u} + \nabla p\|^2_{[L^2(T)]^d}$. So the method simultaneously stabilizes spurious Galerkin solutions of (13) coming from dominating advection and violation of the discrete inf-sup condition (14).

*Remark 3.1.* A crucial point in the numerical analysis is the Galerkin orthogonality

$$\mathcal{A}_{rbs}(\mathbf{b}; U - U_h, V_h) = 0 \qquad \forall V_h \in \mathbf{W}_h^{r,s}. \tag{18}$$

Other residual-based variants, containing the SUPG-/PSPG-stabilization with $\delta_T = \delta_T^u = \delta_T^p$, are the Galerkin/ Least-squares (GLS) method [14] and the Douglas/Wang- or algebraic subgrid-scale (ASGS) method [12] adding

$$\sum_{T\in\mathcal{T}_h} (L_{Os}(\mathbf{b}; U) - \mathbf{f}, \delta_T L_{Os}(\mathbf{b}; V))_T$$

and

$$-\sum_{T\in\mathcal{T}_h}\left(L_{Os}(\mathbf{b};U)-\mathbf{f},\delta_T L^*_{Os}(\mathbf{b};V)\right)_T,$$

respectively, to the Galerkin formulation (13). The analysis of these methods is similar to the SUPG/PSPG/grad-div scheme. □

For details and full proofs of the following presentation, we refer to [29] and [2].

### 3.1 Quasi-optimal estimates on arbitrary meshes

The subsequent analysis provides existence, uniqueness and a generalized result of Cea type for the discrete solution without geometrical conditions on the mesh. Stability of the residual-based method (15)-(17) with $\delta_T = \delta_T^u = \delta_T^p$ is proved w.r.t.

$$[\![V]\!]^2_{rbs} := \|\nu^{\frac{1}{2}}\nabla\mathbf{v}\|^2_{L^2(\Omega)} + \|c^{\frac{1}{2}}\mathbf{v}\|^2_{L^2(\Omega)} + J_{rbs}(V,V), \tag{19}$$

$$J_{rbs}(V,V) := \sum_T \delta_T\|(\mathbf{b}\cdot\nabla)\mathbf{v}+\nabla q\|^2_{L^2(T)} + \sum_T \gamma_T\|\nabla\cdot\mathbf{v}\|^2_{L^2(T)} \tag{20}$$

with parameters $\delta_T, \gamma_T$ to be determined. A simplified analysis is possible since $[\![\cdot]\!]_{rbs}$ is a mesh-dependent norm on $\mathbf{W}_h^{r,s}$ if $\delta_T > 0$.

Consider a (possibly anisotropic) element $T \subset \mathbb{R}^d$, $d = 2, 3$, with sizes $h_{1,T} \geq \ldots \geq h_{d,T}$. A key point in the stability analysis is the local inverse inequality

$$\|\Delta\mathbf{w}\|_{[L^2(T)]^d} \leq \mu_{inv} h_{d,T}^{-1}\|\nabla\mathbf{w}\|_{[L^2(T)]^{d\times d}} \quad \forall\mathbf{w}\in\mathbf{V}_h^r. \tag{21}$$

to bound the term $\Delta\mathbf{u}_h$ in the SUPG-term in (16). Assume that the conditions

$$0 < \delta_T \;\leq\; \frac{1}{2}\min\left\{\frac{h_{d,T}^2}{\mu_{inv}^2\nu}; \frac{1}{c}\right\}, \quad 0 \leq \gamma_T. \tag{22}$$

on the stabilization parameters are satisfied. In view of (21), the upper bound of the stabilization parameter $\delta_T$ is related to $h_{d,T}$. The inverse inequality (21) and (22) imply that the bilinear form $\mathcal{A}_{rbs}(\mathbf{b};\cdot,\cdot)$, defined in (16), satisfies

$$\mathcal{A}_{rbs}(\mathbf{b};W_h,W_h) \geq \frac{1}{2}[\![V_h]\!]^2_{rbs}, \qquad \forall W_h \in \mathbf{W}_h^{r,s}. \tag{23}$$

This implies existence and uniqueness of the discrete solution of (15)-(17).

The following continuity result is derived using standard inequalities. It reflects the effect of stabilization with assumption (22): For each $U \in \mathbf{W}$ with $\Delta\mathbf{u}|_T \in [L^2(T)]^d\ \forall T \in \mathcal{T}_h$ and $V_h \in \mathbf{W}_h^{r,s}$ there holds

$$\mathcal{A}_{rbs}(\mathbf{b};U,V_h) \;\preceq\; \mathcal{Q}_{rbs}(U)\ [\![V_h]\!]_{rbs} \tag{24}$$

with

$$\mathcal{Q}_{rbs}(U) := [\![U]\!]_{rbs} + \Big(\sum_{T\in\mathcal{T}_h}\frac{1}{\delta_T}\|\mathbf{u}\|^2_{L^2(T)}\Big)^{\frac12} + \Big(\sum_{T\in\mathcal{T}_h}\frac{1}{\max(\nu,\gamma_T)}\|p\|^2_{L^2(T)}\Big)^{\frac12} + \Big(\sum_{T\in\mathcal{T}_h}\delta_T\|-\nu\Delta\mathbf{u}+c\mathbf{u}\|^2_{L^2(T)}\Big)^{\frac12}. \quad (25)$$

The $L^2$-terms in (25) explode for $\nu, c \to 0$ and vanishing stabilization with $\delta_T = \gamma_T = 0$.

The standard combination of the stability and continuity estimates (23) and (24) with Galerkin orthogonality (18) leads to the desired error estimate of Cea-type. Consider solutions $U \in \mathbf{W}$ and $U_h \in \mathbf{W}_h^{r,s}$ of the continuous and of the discrete problem, respectively. Let $\{I^u_{h,r}\mathbf{u}, I^p_{h,s}p\} \in \mathbf{W}_h^{r,s}$ be an appropriate interpolant of $U$, e.g., the Lagrange interpolant. Then we obtain an a-priori estimate of Cea-type for the scheme (15)-(17):

$$[\![U-U_h]\!]_{rbs} \preceq \mathcal{Q}_{rbs}(\{\mathbf{u}-I^u_{h,r}\mathbf{u}, p-I^p_{h,s}p\}). \quad (26)$$

It remains to evaluate the right hand side of (26) using appropriate interpolation estimates and to fix the parameter sets $\{\delta_T\}$ and $\{\gamma_T\}$.

### 3.2 $L^2$-control of pressure

The previous result provides no control of the $L^2$-norm of the pressure. Therefore we analyze the stabilized method (15)-(17) w.r.t. the norm

$$|\!|\!|V|\!|\!|_{rbs} := \Big([\![V]\!]^2_{rbs} + \sigma\|q\|^2_{L^2(\Omega)}\Big)^{\frac12} \quad (27)$$

with parameter $\sigma$ to be determined.

#### 3.2.1 Shape-regular meshes:

Suppose first that the triangulation $\mathcal{T}_h$ is *shape-regular*, i.e., there exists a constant $C_{sh}$, independent of the meshsize $h$ with $h_T = h|_T$, such that $C_{sh}h_T^d \le \mathrm{meas}(T)$ for all $T \in \cup_h\mathcal{T}_h$. In particular, this excludes anisotropic elements. The inverse constant in (21) reads $\mu_{inv} = \tilde{\mu}_{inv}r^2$. Assume now additionally

$$0 < \mu_0\frac{h_T^2}{r^2} \le \delta_T \le \frac12\min\left\{\frac{h_T^2}{\tilde{\mu}^2_{inv}r^4\nu}; \frac{1}{\|c\|_{L^\infty(T)}}\right\}, \quad 0 \le \delta_T\|\mathbf{b}\|^2_{L^\infty(T)} \le \gamma_T. \quad (28)$$

Taking advantage of Verfürth's trick, cf. [32], we can show that there exists a constant $\beta > 0$, independent of all critical parameters $(\nu, c, h, r, s)$ such that the bilinear form $\mathcal{A}_{rbs}(\mathbf{b};\cdot,\cdot)$ satisfies

$$\inf_{U_h\in\mathbf{W}_h^{r,s}}\sup_{V_h\in\mathbf{W}_h^{r,s}}\frac{\mathcal{A}_{rbs}(\mathbf{b};U_h,V_h)}{|\!|\!|U_h|\!|\!|_{rbs}|\!|\!|V_h|\!|\!|_{rbs}} \ge \beta \quad (29)$$

with the weight

$$\sqrt{\sigma} \sim \left( \sqrt{\gamma} + \frac{1}{\mu_0} + \sqrt{\nu} + \sqrt{c} C_F + \frac{C_F \|\mathbf{b}\|_{L^\infty(\Omega)}}{\sqrt{\nu + c C_F^2}} + \max_T \frac{h_T \|\mathbf{b}\|_{L^\infty(T)}}{\sqrt{\nu}} \right)^{-1} \tag{30}$$

of the $L^2$-norm of the pressure in (27). Moreover, it denotes $\gamma = \max_{T \in \mathcal{T}_h} \gamma_T$ and $C_F$ the Friedrichs constant. Note that $\sigma$ is only used for the analysis.

A combination of the modified inf-sup stability result (29) with Galerkin orthogonality (18) and (24) leads to the improved quasi-optimal estimate of Cea type

$$\|U - U_h\|_{rbs} \preceq \mathcal{Q}_{rbs}(\{\mathbf{u} - I^u_{h,r}\mathbf{u}, p - I^p_{h,s} p\}) \tag{31}$$

with $\mathcal{Q}_{rbs}(\cdot)$ from (25).

*Remark 3.2.* The lower bound of $\delta_T$ in (28) can be removed in case of div-stable velocity-pressure interpolations. But then one has to replace the constant $\beta$ in (29) by the inf-sup constant $\beta_0 = \beta_0(r,s)$ from (14). □

### 3.2.2 Hybrid meshes:

Of practical interest are *hybrid* meshes with *anisotropic* mesh refinement of tensor product type (in the sense of [1, Chap. 3]) in the boundary layer and a smooth transition to (in general unstructured) shape-regular (isotropic) meshes away from the layer. We restrict ourselves to the case that the boundary layer is located at the hyperplane $x_d = 0$.

The advantage of this class of meshes is not only that the coordinate transformation is simplified in regions with anisotropic elements but also that certain edges/faces of the elements are orthogonal/parallel to coordinate axes. This is exploited in the analysis. Fig. 1 shows examples of such meshes for the two- and three-dimensional case.

Meshes of tensor product type in the boundary layer region consist of affine elements of tensor product type. That means the transformation of a reference element $\hat{T}$ to the element $T$ shall have (block) diagonal form,

$$x \;=\; \left( \begin{array}{c:c} A_T & 0 \\ \hdashline 0 & \pm h_{d,T} \end{array} \right) \hat{x} + \mathbf{a}_T \quad \text{for } , \tag{32}$$

where $\mathbf{a}_T \in \mathbb{R}^d$, $A_T = \pm h_{1,T}$ for $d = 2$ and $A_T \in \mathbb{R}^{2\times 2}$ for $d = 3$ with $|\det A_T| \sim h_{1,T}^2$, $\|A_T\| \sim h_{1,T}$, $\|A_T^{-1}\| \sim h_{1,T}^{-1}$. In this way the element sizes $h_{1,T}, \ldots, h_{d,T}$ are implicitly defined. Note that the additional conditions yield $h_{1,T} \sim h_{2,T}$ for $d = 3$.

Under these assumptions, the triangles/tetrahedra can be grouped into pairs/triples which form a rectangle/triangular prism of tensor product type. We demand further that there is no abrupt change in the element sizes, that means $h_{i,T} \sim h_{i,T'}$ for all $T'$ with $\overline{T} \cap \overline{T'} \neq \emptyset$, $i = 1, \ldots, d$. This implies that the transition region between the structured mesh

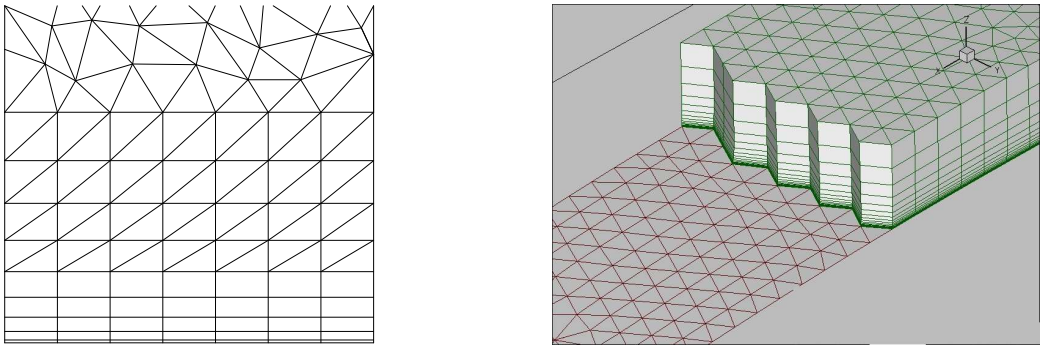

Figure 1: Examples of hybrid meshes in the two- and three-dimensional case

in the boundary layer zone and the unstructured mesh consists of isotropic elements only. In particular, Shishkin's piecewise equidistant meshes in boundary layers are excluded.

Here, we consider *equal-order* interpolation, i.e., $r = s \geq 1$. Condition (28) reads now

$$0 < \mu_0 h_{1,T}^2 \leq \delta_T \leq \frac{1}{2} \min \left\{ \frac{h_{d,T}^2}{\mu_{inv}^2 \nu}; \frac{1}{c} \right\}, \quad 0 \leq \delta_T \|\mathbf{b}\|_{[L^\infty(T)]^d}^2 \leq \gamma_T. \tag{33}$$

with some constant $\mu_0 > 0$ (see Remark 3.3). Then there exists a positive constant $\beta$, independent of of all important parameters ($\nu$, $c$, $h_{1,T}, \ldots, h_{d,T}$, aspect ratio, $\delta_T$, $\gamma_T$) such that the modified inf-sup condition (29) is again satisfied, here for the FE pair $\mathbf{W}_h^{r,r} = \mathbf{V}_h^r \times \mathbf{Q}_h^r$. A combination of (29) with the continuity estimate (24) leads again to the modified quasi-optimal estimate (31) of Cea type.

*Remark 3.3.* The lower bound of $\delta_T$ in assumption (33) implicitly implies

$$\sqrt{\mu_0} \max_{T \in \mathcal{T}_h} \frac{h_{1,T}}{h_{d,T}} \leq \frac{1}{\mu_{inv} \sqrt{2\nu}} \tag{34}$$

with a restriction on the aspect ratio of $T$. A reasonable choice in boundary layers at a wall is $h_{d,T} \geq \sqrt{\nu} h_{1,T}$; thus guaranteeing that $\mu_0 = \mathcal{O}(1)$, see also Sect. 3.3.2. □

### 3.3 A-priori error estimates

The next goal is to specify the quasi-optimal error estimates (26) and/or (31) of Cea-type using local interpolation inequalities and to fix the stabilization parameters $\delta_T, \gamma_T$. For simplicity, we assume that the solution $U \in \mathbf{W} := \mathbf{V} \times \mathbf{Q}$ of (8)-(10) is smooth enough such that $\{I_{h,r}^u \mathbf{u}, I_{h,s}^p p\} \in \mathbf{W}_h^{r,s}$ can be chosen as the global Lagrange interpolants of $\{\mathbf{u}, p\}$.

#### 3.3.1 Shape-regular meshes:

On a *shape-regular* mesh, we can apply the local interpolation result

$$\|v - I_{h,r}^T v\|_{H^m(T)} \leq C_I \frac{h_T^{l-m}}{r^{k-m}} \|v\|_{H^k(T)}, \quad 0 \leq m \leq l = \min(r+1, k) \tag{35}$$

for the Lagrange interpolation $I_{h,r}^T v$ of $v \in H^k(T)$ with $k > \frac{d}{2}$, [19], Sect. 4. Here $C_I$ is a constant independent of $h_T, r, v, T$ but dependent on $m, k, C_{sh}$. Based on the quasi-optimal a-priori estimate (26) and/or (31) and on the assumption (22), we obtain

$$\|\!|U - U_h|\!\|_{rbs}^2 \preceq \sum_{T\in\mathcal{T}_h} \left( M_T^u \frac{h_T^{2(l_u-1)}}{r^{2(k_u-1)}} \|\mathbf{u}\|_{H^{k_u}(T)}^2 + M_T^p \frac{h_T^{2(l_p-1)}}{s^{2(k_p-1)}} \|p\|_{H^{k_p}(T)}^2 \right) \tag{36}$$

with $l_u := \min\{r+1, k_u\}$, $l_p := \min\{s+1, k_p\}$ and

$$\begin{aligned} M_T^u &= \frac{h_T^2}{r^2\delta_T} + \delta_T \left( \frac{\|c\|_{L^\infty(T)}^2 h_T^2}{r^2} + \|\mathbf{b}\|_{L^\infty(T)}^2 + \frac{r^2\nu^2}{h_T^2} \right) + \gamma_T + \nu + \frac{\|c\|_{L^\infty(T)} h_T^2}{r^2}, \\ M_T^p &= \delta_T + \frac{h_T^2}{s^2 \max(\nu, \gamma_T)}. \end{aligned}$$

(i) *Equal-order interpolation of velocity and pressure* ($r = s \in \mathbb{N}$):

Such pairs do not fulfill the discrete inf-sup condition (14). The equilibration of the $\delta_T$- and $\gamma_T$-dependent terms in $M_T^u$ and $M_T^p$ together with the stability conditions (22), (28) yields

$$\delta_T \sim \min\left\{ \frac{h_T^2}{r^4\nu}; \frac{h_T}{r\|\mathbf{b}\|_{L^\infty(T)}}; \frac{1}{\|c\|_{L^\infty(T)}} \right\}, \qquad \gamma_T \sim \frac{h_T^2}{r^2\delta_T}. \tag{37}$$

Then, a sufficiently smooth solution $U$ of (8)-(10) with $U|_T \in [H^k(T)]^d \times H^k(T)$ for each $T \in \mathcal{T}_h$, obeys the error estimate (with $l = \min(r+1, k)$)

$$\|\!|U - U_h|\!\|_{rbs}^2 \preceq \sum_{T\in\mathcal{T}_h} \frac{h_T^{2(l-1)}}{r^{2(k-1)}} M_T \left( \|\mathbf{u}\|_{H^k(T)}^2 + \|p\|_{H^k(T)}^2 \right), \tag{38}$$

$$M_T = \nu r^2 + \frac{\|\mathbf{b}\|_{L^\infty(T)} h_T}{r} + \frac{\|c\|_{L^\infty(T)} h_T^2}{r^2}. \tag{39}$$

*Remark 3.4.* Estimate (38) is optimal w.r.t. $h_T$. It is suboptimal in the spectral order $r$ in a transition region between the diffusion-dominated and the advection-dominated limits. This is caused by the term $\frac{r^4\nu}{h_T^2}$ in (37) in order to fulfill the stability conditions (28). It is possible to refine the $L^2$-term of $\mathbf{u}$ on the right hand side of (25), thus giving an optimal estimate w.r.t. $r$ at least in the diffusion-dominated limit, see [29]. □

(ii) *Interpolation pairs* $\mathbf{V}_h^r \times \mathbf{Q}_h^s$ *with* $r = s + 1$:

This includes the div-stable Taylor-Hood pairs with $s = r - 1 \in \mathbb{N}$ on a shape-regular mesh $\mathcal{T}_h$. (An extension to $r \geq s + 1$ is straightforward.) A balance of the $\gamma_T$- and $\delta_T$-dependent terms in $M_T^u$ and $M_T^p$ yields

$$\gamma_T = \nu + \gamma, \ \gamma \sim 1, \qquad \delta_T \sim \frac{h_T^2}{\gamma_0 r^2}. \tag{40}$$

In this case, a sufficiently smooth solution $U$ of the Oseen problem (8)-(10) with $U|_T \in [H^{k+1}(T)]^d \times H^k(T)$ for each $T \in \mathcal{T}_h$ obeys the error estimate

$$\|U - U_h\|_{rbs}^2 \preceq \sum_{T\in\mathcal{T}_h} \frac{h_T^{2l}}{s^{2k}} \left( \|\mathbf{u}\|_{H^{k+1}(T)}^2 + \|p\|_{H^k(T)}^2 \right). \tag{41}$$

with $l = \min(r+1, k)$, provided that $\nu + \|\mathbf{b}\|_{L^\infty(T)}^2 h_T^2 r^{-2} + \|c\|_{L^\infty(T)} h_T^2 r^{-2} \le 1$. The latter condition is valid for sufficiently small $h_T$. The estimate (41) is optimal w.r.t. both $h_T$ and $r$. The choice (40) reflects the importance of the grad-div stabilization term and a decreasing influence of the SUPG/PSPG term with increasing spectral order $r$.

### 3.3.2 Hybrid meshes:

Based on the quasi-optimal estimate (26) and/or (31), we derive here error estimates and design the parameters $\delta_T, \gamma_T$ with emphasis on the anisotropy of an element.

Appropriate anisotropic interpolation estimates of the FE spaces $X_h^r$ are required in order to compensate large derivatives in some direction $x_d$ by the small element diameter $h_{d,T}$. We refer to [1] for a basic interpolation theory which relies on some geometrical conditions (maximal angle condition and the coordinate system condition). These conditions are satisfied for the hybrid meshes introduced in Sec. 3.2. The anisotropic interpolation result for the Lagrangian interpolation operator $I_{h,r} : \mathbf{C}(\overline{T}) \to \mathcal{P}_r(T)$ reads as follows, see [1, Chap. 2]: Assume that $v \in W^{\ell,p}(T)$, with $\ell \in \{1, \ldots, r+1\}$, $p \in [1, \infty]$, such that $p > 2/\ell$. Fix $m \in \{0, \ldots, \ell - 1\}$. Then the following estimate holds

$$||v - I_{h,r} v\|_{W^{m,p}(T)} \le C \sum_{|\alpha|=\ell-m} \mathbf{h}_T^\alpha \, \|D^\alpha v\|_{W^{m,p}(T)} \quad \mathbf{h}_T^\alpha := h_1^{\alpha_1} \ldots h_d^{\alpha_d}. \tag{42}$$

Let the assumptions of Sec. 3.2.2 be valid. Moreover, assume that the solution $U = \{\mathbf{u}, p\} \in \mathbf{W}$ is continuous and satisfies $\mathbf{u}|_T \in [H^k(T)]^2$, $p|_T \in H^k(T)$ with $k > 1$ for all $T \in \mathcal{T}_h$. Then, using the notation $l := \min(r, k-1)$ for the convergence order, there exists a constant $C$ independent of all important parameters ($\nu$, $c$, $\mathbf{h}_T$, aspect ratio, $\delta_T$, $\gamma_T$) such that

$$\|U - U_h\|_{rbs}^2 \le C \sum_{T\in\mathcal{T}_h} \sum_{|\alpha|=l} \sum_{|\beta|=1} \mathbf{h}_T^{2\alpha} \left\{ E_{T,\beta}^p \|D^{\alpha+\beta} p\|_{L^2(T)}^2 + E_{T,\beta}^u \|D^{\alpha+\beta}\mathbf{u}\|_{L^2(T)}^2 \right\} \tag{43}$$

with

$$E_{T,\beta}^p = \delta_T + \frac{1}{\nu + \gamma_T} \mathbf{h}_T^{2\beta} \tag{44}$$

$$E_{T,\beta}^u = \nu + c h_{1,T}^2 + \gamma_T + \delta_T \|\mathbf{b}\|_{[L^\infty(T)]^d}^2 + \frac{\mathbf{h}_T^{2\beta}}{\delta_T}. \tag{45}$$

The standard strategy would be to minimize the terms $E^u_{T,\beta}$ and $E^p_{T,\beta}$ elementwise w.r.t. the parameters $\delta_T, \gamma_T$. The mixed character of the problem requires a more careful approach. Let us define $\tilde{h}_T \in [h_{d,T}, h_{1,T}]$. Taking assumption (33) into account, we propose to define the parameters according to

$$\delta_T \sim \min\left(\frac{h^2_{d,T}}{\mu^2_{inv}\nu}; \frac{1}{c}; \frac{\tilde{h}_T}{\|\mathbf{b}\|_{[L^\infty(T)]^d}}\right), \qquad \gamma_T \sim \frac{\tilde{h}^2_T}{\delta_T}. \tag{46}$$

In the isotropic region $\Omega_{iso}$ away from the boundary layer, we set $\tilde{h}_T \sim h_{1,T}$ which leads to the standard design (37), see Sec. 3.3.1. The corresponding error part reduces to

$$\begin{aligned} Err_{iso} \;\leq\; C \sum_{T\in\mathcal{T}_h\cap\Omega_{iso}} \sum_{|\alpha|=l} \sum_{|\beta|=1} h^{2l}_{1,T} \Big\{ \delta_T \|D^{\alpha+\beta} p\|^2_{L^2(T)} \;+ \\ +\; \left(\nu + c h^2_{1,T} + h_{1,T}\|\mathbf{b}\|_{[L^\infty(T)]^d}\right) \|D^{\alpha+\beta}\mathbf{u}\|^2_{L^2(T)} \Big\}. \end{aligned} \tag{47}$$

The parameter design in the boundary layer region $\Omega_{aniso}$ is more involved. We assume that the boundary layer region is located at the hyperplane $x_d = 0$. Prandtl's boundary layer theory for laminar flows starts with an asymptotic ansatz in powers of $\sqrt{\nu}$ such that

$$p = p_0 + \sqrt{\nu} p_1 + \ldots, \qquad u_i = u_{i,0} + \sqrt{\nu} u_{i,1} + \ldots, \quad i = 1, \ldots, d.$$

It is known that $p_0$ varies at most slowly with $x_d$, whereas the components $u_{i,0}$ can have large gradients in $x_d$-direction. This motivates to refine the mesh in $x_d$-direction towards the wall by setting $h_{d,T} \sim g(x_d) h_{1,T}$ with a strongly increasing monitor function $g(\cdot)$ such that $g(x_d) \sim \sqrt{\nu}$ in the mesh layer nearest to the wall and $g(x_d) \sim 1$ in the transition region to the isotropic part of the hybrid mesh. The corresponding error contribution is

$$\begin{aligned} Err_{aniso} \;\leq\; C \sum_{T\in\mathcal{T}_h\cap\Omega_{aniso}} \sum_{|\alpha|=l} \sum_{|\beta|=1} \mathbf{h}^{2\alpha}_T \Big\{ \delta_T \left(1 + \frac{\mathbf{h}^{2\beta}_T}{\tilde{h}^2_T}\right) \|D^{\alpha+\beta} p\|^2_{L^2(T)} \;+ \\ +\; \left(\nu + c h^2_{1,T} + \tilde{h}_T \|\mathbf{b}\|_{[L^\infty(T)]^d} + \frac{\max(\tilde{h}^2_T; \mathbf{h}^{2\beta}_T)}{\delta_T}\right) \|D^{\alpha+\beta}\mathbf{u}\|^2_{L^2(T)} \Big\}. \end{aligned} \tag{48}$$

The velocity error part contains the critical term $\frac{h^{2\beta}_T}{\delta_T}$. A careful discussion in [2] shows that it is at most of order $\mathcal{O}(1)$ in the mesh layer nearest to the wall at $x_d = 0$ since $h_{d,T} \sim \sqrt{\nu} h_{1,T}$. Moreover, we observe that the stabilization parameters $\delta_T$ and $\gamma_T$ do not deteriorate in this layer for small $\nu$, thus still preserving $L^2$ control of the pressure.

An increasing value $\tilde{h}_T$ leads to an increasing $\gamma_T$, thus giving improved control of the divergence constraint $\nabla \cdot \mathbf{u}$. On the other hand, the control parameter $\sigma$ of $\|p - p_h\|_{L^2(\Omega)}$ behaves like $1/\sqrt{\sigma} \leq \max_T \sqrt{\gamma_T}$, i.e., the control of this norm gets worse with enlarged $\gamma_T$. Our favoured choice is

$$\tilde{h}_T = (\mathrm{meas}(T))^{\frac{1}{d}}, \tag{49}$$

as a reasonable compromise to balance control of pressure and of divergence. Different variants have been considered in the experiments in [13] too, with no clear preference.

### 3.4 Critical evaluation of residual-based stabilization

A striking advantage of the residual-based stabilization techniques presented in Section 3 is that the a-priori analysis is almost complete for the generalized Oseen problem.

Another major advantage of the residual-based stabilization methods is the compactness of the finite element stencil. The system matrices of the Galerkin FEM and the SUPG/PSPG-stabilized scheme have the form

$$\begin{pmatrix} A & B^T \\ B & 0 \end{pmatrix} \qquad \text{and} \qquad \begin{pmatrix} A_{rbs} & B_1 \\ B_2 & C \end{pmatrix},$$

respectively, with $B_1 \neq B_2$, $C \neq 0$. The blocks $A$ and $A_{rbs}$ as well as $B$, $B_1$ and $B_2$ have a similar sparsity pattern. Thus, the SUPG/PSPG method can be easily incorporated into an existing code for solving the Galerkin FEM. One has to store one additional off-diagonal block and the additional sparse matrix $C$ for the pressure couplings arising from the term $\sum_{T\in\mathcal{T}_h}(\nabla p, \delta_T^p \nabla q)_T$ in the stabilization.

Besides the advantages and the well-developed analysis of the residual-based stabilization methods, there are also some critical points:
The basic problem is the strong coupling of velocity and pressure in the stabilization terms. In particular, the physical meaning of stabilization term $\sum_T \delta_T \|(\mathbf{b}\cdot\nabla)\mathbf{u} + \nabla p\|^2_{L^2(T)}$ is not clear. Assembling of the (full) stabilization terms is rather expensive in 3D. Moreover, second-order derivatives of the velocity have to be evaluated if $r \geq 2$. Another drawback is that the local inverse estimates (to bound second-order derivatives) lead to unpleasant upper bounds of $\delta_T$. Finally, the construction of efficient and robust algebraic preconditioners seems to be not fully solved.

## 4 TOWARDS SYMMETRIC STABILIZATION

A natural question is whether the pressure stabilization (PSPG) is necessary for div-stable interpolation pairs $\mathbf{V}_h^r \times \mathbf{Q}_h^s$, i.e., pairs fulfilling the inf-sup condition (14). Recently, a *reduced stabilized* scheme, by omitting the PSPG terms $\sum_{T\in\mathcal{T}_h}(L_{Os}(\mathbf{b};\mathbf{u},p)-\mathbf{f},\ \delta_T\nabla q)_T$ from scheme (15)-(17), has been analyzed in [15]:

$$\text{find } U=(\mathbf{u},p)\in \mathbf{V}_h^r\times\mathbf{Q}_h^s,\ \text{s.t.}\ \ \mathcal{A}_{rss}(\mathbf{b};U,V) \ = \ \mathcal{L}_{rss}(V) \quad \forall\, V\in\mathbf{V}_h^r\times\mathbf{Q}_h^s. \tag{50}$$

with

$$\begin{aligned} \mathcal{A}_{rss}(\mathbf{b};U,V) &:= \mathcal{A}(\mathbf{b};U,V) + \sum_{T\in\mathcal{T}_h}\gamma_T\,(\nabla\cdot\mathbf{u},\nabla\cdot\mathbf{v})_T + \sum_{T\in\mathcal{T}_h}(L_{os}(\mathbf{b},\mathbf{u},p),\delta_T^u(\mathbf{b}\cdot\nabla)\mathbf{v})_T \\ \mathcal{L}_{rss}(V) &:= \mathcal{L}(V) + \sum_{T\in\mathcal{T}_h}(\mathbf{f},\delta_T^u(\mathbf{b}\cdot\nabla)\mathbf{v})_T. \end{aligned}$$

The analysis in [15] is given for *quasi-uniform* meshes and under the assumption

$$\exists\kappa>0 \ \text{ such that } \ \nu + ch_T^2 \geq \kappa h_T^2. \tag{51}$$

*Remark 4.1* Condition (51) is quite natural in case of implicit time stepping for the Navier-Stokes model (1)-(2) with time steps $\tau \sim \frac{1}{c}$ with $\tau \preceq 1$. □

There exists a constant $\beta > 0$ with $\beta \neq \beta(h, r, s, \nu, \tau)$ such that the modified inf-sup stability condition

$$\inf_{W_h \in \mathbf{W}_h^{r,s}} \sup_{V_h \in \mathbf{W}_h^{r,s}} \frac{\mathcal{A}_{rss}(\mathbf{b}; W_h, V_h)}{\|W_h\|_{rss}\|V_h\|_{rss}} \geq \beta \tag{52}$$

is proved using the following stabilized norm

$$\begin{aligned} \|V\|_{rss} &:= \Big( \|\sqrt{\nu}\nabla \mathbf{v}\|^2_{L^2(\Omega)} + \|\sqrt{c}\mathbf{v}\|^2_{L^2(\Omega)} + \sigma_r \|\nabla q\|^2_{L^2(\Omega)} \\ &\quad + \sum_T \gamma_T \|\nabla \cdot \mathbf{v}\|^2_{L^2(T)} + \sum_T \delta_T \|\mathbf{b} \cdot \nabla \mathbf{v}\|^2_{L^2(T)} \Big)^{\frac{1}{2}}. \end{aligned} \tag{53}$$

A similar analysis, as sketched in Sec. 3.3.1, yields the following design

$$\gamma_T \sim \nu + \gamma, \ \gamma \sim 1; \qquad \delta_T^u \sim \frac{h_T^2}{r^2}, \qquad \delta_T^p = 0 \tag{54}$$

and

$$\|U - U_h\|_{rss} \preceq \sum_{T \in \mathcal{T}_h} \left( \frac{h_T^{2l}}{s^{2k}} \|p\|^2_{H^k(T)} + \frac{h_T^{2l}}{r^{2k}} \|\mathbf{u}\|^2_{H^{k+1}(T)} \right). \tag{55}$$

Surprisingly, numerical experiments for the fully stabilized scheme of Sec. 3 and the corresponding reduced stabilized scheme (50) with Taylor-Hood elements $P_{k+1}/P_k$ give quasi-optimal and almost identical results. Another important observation is that the grad-div stabilization terms are really necessary for $0 < \nu \ll 1$. Moreover, an order reduction of $\frac{1}{2}$ is observed in the error estimates if the standard design for SUPG/PSPG in case of equal-order interpolation, i.e., according to (37), is used instead of (54).

Further numerical results in [15] show that SUPG stabilization is useful for problems with boundary and/or interior layers. Moreover, corresponding experiments for laminar Navier-Stokes flows (driven cavity and backward facing step in 2D) show that these observations remain valid in the nonlinear case too.

*Remark 4.2.* A recent result by Matthies [30] is devoted to the general residual-based stabilized scheme (15)-(17) containing the three parameter sets $\{\delta_T^u\}$, $\{\delta_T^p\}$ and $\{\gamma_T\}$ with $0 \leq \delta_T^p \leq \delta_T^u$. For the case of div-stable pairs $\mathbf{W}_h^{r,s}$, the analysis is given w.r.t. the norm

$$\|V\|_s^2 := \|\nu^{\frac{1}{2}}\nabla \mathbf{v}\|^2_{L^2(\Omega)} + \|c^{\frac{1}{2}}\mathbf{v}\|^2_{L^2(\Omega)} + \sigma \|p\|^2_{L^2(\Omega)} + \sum_T \delta_T^p \|\nabla p\|^2_{H^1(T)} + J_s(V, V), \tag{56}$$

$$J_s(V, V) := \sum_T \left( \delta_T^u \|(\mathbf{b} \cdot \nabla)\mathbf{v}\|^2_{L^2(T)} + \delta_T^p \|\nabla q\|^2_{L^2(T)} + \gamma_T \|\nabla \cdot \mathbf{v}\|^2_{L^2(T)} \right). \tag{57}$$

Under a condition similar to (51), one obtains the a-priori estimate (55) provided that the parameters are chosen according to (54) but for $\delta_T^p \in [0, \delta_T^u]$. In particular, this generalizes the result for the reduced stabilized scheme (50) above. Moreover, the restriction to quasi-uniform meshes can be removed. □

## 5 SYMMETRIC STABILIZATION TECHNIQUES

Some drawbacks of the classical stabilization methods presented in Sec. 3 stem from the strong velocity-pressure coupling in the stabilization terms. Here, we will consider techniques with decoupled *symmetric* stabilization terms which avoid this problem. Such methods loose the Galerkin orthogonality. The subgrid-viscosity concept [17] and the variational multiscale method [20] provide some ideas for the construction of such schemes.

### 5.1 Coupled vs. decoupled stabilization

The starting point is the SUPG/PSPG stabilization term of equation (16)

$$\sum_{T\in\mathcal{T}_h} (L_{Os}(\mathbf{b};\mathbf{u},p),\ \delta_T^u(\mathbf{b}\cdot\nabla)\mathbf{v}+\delta_T^p\nabla q)_T\,.$$

The subgrid viscosity concept [17] leads to the idea that the stabilization of the residual does not have to act on the whole residual but only on its projection into some appropriate subspace. Consider an abstract projection operator $(I-P)$ and the modified stabilization term

$$\sum_{T\in\mathcal{T}_h} \Big((I-P)L_{Os}(\mathbf{b};\mathbf{u},p),\ (I-P)\Big(\delta_T^u(\mathbf{b}\cdot\nabla)\mathbf{v}+\delta_T^p\nabla q\Big)\Big)_T \tag{58}$$

(with a similar modification of the right hand side of the equation). Taking now $\mathbf{v}=\mathbf{u}$, $q=p$ and (for simplicity) $\delta_T=\delta_T^u=\delta_T^p$, one observes that (58) becomes

$$\begin{aligned}\sum_{T\in\mathcal{T}_h} \Big\{&((I-P)(-\nu\Delta\mathbf{u}+c\mathbf{u}),\delta_T(I-P)((\mathbf{b}\cdot\nabla)\mathbf{u}+\nabla p))_T\\ &+\|(\delta_T)^{\frac12}(I-P)((\mathbf{b}\cdot\nabla)\mathbf{u}+\nabla p)\|^2_{L^2(T)}\Big\}.\end{aligned} \tag{59}$$

The first part of (59) is necessary for consistency, the last part gives positivity. If the operator $(I-P)$ is chosen in such a way that the first (consistency) part vanishes sufficiently fast as $h\to 0$, then it could be dropped without spoiling the rate of convergence. Then one may also drop the Petrov-Galerkin type modification of the right hand side.

Moreover, the positive part may be split again in order to decouple velocities and pressure. Introducing separate stabilization terms for pressure and velocity does not change the consistency properties of the scheme since the weak consistency is given by the approximation properties of the projection and not by the residual. Then, (58) is transformed to the decoupled and symmetric form

$$\sum_{T\in\mathcal{T}_h} (\delta_T^u(I-P)((\mathbf{b}\cdot\nabla)\mathbf{u}),(I-P)((\mathbf{b}\cdot\nabla)\mathbf{v}))_T+(\delta_T^p(I-P)\nabla p,(I-P)\nabla q)_T\,. \tag{60}$$

A similar argument can be applied to the grad-div stabilization term.

Choosing the subspaces and the projection operators in a specific way, we obtain different stabilization techniques below where we will use for the stabilized bilinear form the unified notation

$$\mathcal{A}(\mathbf{b};U,V)+\mathcal{S}_*(\mathbf{b};U,V). \tag{61}$$

### 5.2 An example: Local projection-based stabilization method

A typical example for a scheme of type (61) is given by the *local projection-based* stabilization method [4] which is designed so far for *equal-order* interpolation ($r=s$) and stabilization of advective terms.

The method requires a two-level data structure. We assume a global coarsening of the basic mesh $\mathcal{T}_h$ giving the coarse mesh $\mathcal{T}_{2h}$. Then we consider the space of patch-wise *discontinuous* finite elements of degree $r-1$:

$$\overline{X}_{2h}^{r-1} := \{v\in L^2(\bar\Omega) \mid \ v|_T\circ F_T\in P_{r-1}(\hat T)\ \forall T\in\mathcal{T}_{2h}\}$$

and the local $L^2-$projection $P_{lps}:\ X_h^r\to\overline{X}_{2h}^{r-1}$, such that

$$(\phi-P_{lps}\phi,\psi)\ =\ 0\quad\forall\phi\in X_h^r\quad\forall\psi\in\overline{X}_{2h}^{r-1}.$$

Finally, we define the fluctuation operator $\bar\varkappa_h\ =\ I-P_{lps}$. w.r.t. $P_{lps}$. The stabilized bilinear form with symmetric and decoupled stabilization terms is defined according to

$$\begin{aligned}\mathcal{A}_{lps}(\mathbf{b};U,V) &:= \mathcal{A}(\mathbf{b};U,V)+\mathcal{S}_{lps}(U,V), &(62)\\ \mathcal{S}_{lps}(U,V) &:= \underbrace{(\bar\varkappa_h\nabla p,\delta^p\bar\varkappa_h\nabla q)}_{pressure\quad stab.}+\underbrace{(\bar\varkappa_h\nabla\cdot\mathbf{u},\gamma\bar\varkappa_h\nabla\cdot\mathbf{v})}_{divergence\quad stab.}+\underbrace{(\bar\varkappa_h\nabla\mathbf{u},\delta^u\bar\varkappa_h\nabla\mathbf{v})}_{advection\quad stab.}. &(63)\end{aligned}$$

The right hand side remains unchanged such that the discrete problem reads:

$$\text{find } U_h=\{\mathbf{u}_h,p_h\}\in\mathbf{W}_h^{r,s},\ \text{s.t.}\quad \mathcal{A}_{lps}(\mathbf{b};U_h,V)=\mathcal{L}(V)\quad\forall V=\{\mathbf{v},q\}\in\mathbf{W}_h^{r,s}. \tag{64}$$

Due to $L^2$-orthogonality, the stabilization term can be written as

$$\mathcal{S}_{lps}(\mathbf{b};U,V)\ =\ (\bar\varkappa_h\nabla p,\delta^p\nabla q)\ +\ (\bar\varkappa_h(\nabla\cdot\mathbf{u}),\gamma\nabla\cdot\mathbf{v})+(\bar\varkappa_h\nabla\mathbf{u},\delta^u\nabla\mathbf{v})\,.$$

A complete description of the numerical analysis w.r.t. the simplified norm

$$\begin{aligned}[\![V]\!]_{lps}^2 &:= \|\sqrt{\nu}\nabla\mathbf{v}\|_{L^2(\Omega)}^2+\|\sqrt{c}\mathbf{v}\|_{L^2(\Omega)}^2+\sigma\|p\|_{L^2(\Omega)}^2+J_{lps}(V,V), &(65)\\ J_{lps}(V,V) &:= \sum_T\left(\|\sqrt{\delta^p\overline{\varkappa_h}}\nabla q\|_{L^2(\Omega)}^2+\|\sqrt{\delta^u\overline{\varkappa_h}}\nabla\mathbf{v}\|_{L^2(\Omega)}^2+\|\sqrt{\gamma\overline{\varkappa_h}}\nabla\cdot\mathbf{v}\|_{L^2(\Omega)}^2\right). &(66)\end{aligned}$$

together with numerical results for this method can be found in [4]. The error estimates are comparable to the results for the classical residual-based stabilization scheme in Sec. 3.3.1.

*Remark 5.1.* Another example of type (61) is the *edge/face oriented stabilization* method which can be classified as a residual-based stabilization method since it controls the inter-element jumps of the non-symmetric terms in the Oseen equation:

$$\text{find } U_h \in \mathbf{W}_h^{r,r}, \text{ such that } \mathcal{A}_{eos}(\mathbf{b}; U_h, V_h) = \mathcal{L}(V_h) \ \forall\, V_h = \{\mathbf{v}_h, q_h\} \in \mathbf{W}_h^{r,r} \tag{67}$$

with

$$\begin{aligned} \mathcal{A}_{eos}(\mathbf{b}; U_h, V_h) &:= \mathcal{A}(\mathbf{b}; U_h, V_h) + \mathcal{S}_{eos}(\mathbf{b}; U_h, V_h), && (68)\\ \mathcal{S}_{eos}(\mathbf{b}; U_h, V_h) &:= \sum_{e\in\mathcal{E}} \int_e \Big\{ \gamma_e^u(\mathbf{b}, h_e)[\nabla \mathbf{u}_h \mathbf{n}_e] \cdot [\nabla \mathbf{v}_h \mathbf{n}_e] && (69)\\ &+ \gamma_e(\mathbf{b}, h_e)[\nabla \cdot \mathbf{u}_h][\nabla \cdot \mathbf{v}_h] + \gamma_e^p(\mathbf{b}, \nu, h_e)[\nabla p_h \cdot \mathbf{n}_e][\nabla q_h \cdot \mathbf{n}_e] \mathrm{d}s \Big\}. \end{aligned}$$

The numerical analysis for the case of equal-order velocity-pressure aproximation $\mathbf{W}_h^{r,r}$ is given in [8]. The application to inf-stable pairs $\mathbf{W}_h^{r,s}$ can be found in [9]. □

### 5.3 General framework of projection-based methods

Here we want to give a more general framework of *projection-based* methods on a two-level data structure with a coarse grid $\mathcal{T}_H$ and a fine grid $\mathcal{T}_h$ with $H > h$. Denote by $\mathbf{G}_{H,U}$ the coarse or large scale space of $d+1$ gradient fields and by $\delta \geq 0$ an additional viscosity. An abstract projection-based scheme is:

$$\text{find } \{U_h, \mathbb{G}_{H,U}\} \equiv \{\mathbf{u_h}, p_h, \mathbb{G}_{H,U}\} \in \mathbf{W}_h^{r,s} \times \mathbf{G}_{H,U} \quad \text{s.t.} \tag{70}$$

$$\begin{aligned} \mathcal{A}(\mathbf{b}; U_h, V_h) + (\nabla U_h - \mathbb{G}_{H,U}, \delta \nabla V_h) &= \mathcal{L}(V_h) \quad \forall\, V_h \in \mathbf{W}_h^{r,s},\\ (\nabla U_h - \mathbb{G}_{H,U}, \mathbb{L}_{H,U}) &= 0 \qquad \forall\, \mathbb{L}_{H,U} \in \mathbf{G}_{H,U}, \end{aligned} \tag{71}$$

i.e., with $L^2(\Omega)$ projection of pressure and velocity gradients into $\mathbf{G}_{H,U}$. The trivial choice

$$\mathbf{G}_{H,U} = (\nabla \mathbf{V}_h^r) \times (\nabla \mathbf{Q}_h^s) \tag{72}$$

where, e.g., $\nabla \mathbf{V}_h^r$ stands for a space consisting of all derivatives of functions in space $\mathbf{V}_h^r$, avoids any projection. This way we obtain the standard Galerkin scheme (13).

(i) *Projection-based stabilization with equal-order ansatz for velocity-pressure:*
Consider an equal-order ansatz for velocity-pressure, i.e., $\mathbf{W}_h^{r,r} = \mathbf{V}_h^r \times \mathbf{Q}_h^r$. The choice

$$\mathbf{G}_{H,U} := (\nabla \mathbf{V}_h^r) \times (X_h^r)^d \tag{73}$$

leads to *global projection* methods. Codina/Blasco [11] proposed for the Stokes model that the gradient of the velocity is not projected, but that the pressure gradient is projected onto the discrete velocity space with natural boundary conditions. Such a projection acts globally since $\mathbf{G}_{H,U} \subset (C(\overline{\Omega})^{d\times(d+1)}$.

Let us consider now $\mathbf{G}_{H,U}$ as a discontinuous space, thus leading to *local projection methods:* We use the notation of Section 5.2. The main benefit is that a local condensation of $\mathbb{G}_{H,U}$ is possible now. An example is given by

$$\mathbf{G}_{H,U} := (\overline{X}_{2h}^{r-1})^{d\times d} \times (\overline{X}_{2h}^{r-1})^{d} \tag{74}$$

which leads to $\mathbb{G}_{H,U} = P_{lps}(\nabla U_h)$. Using the $L^2$-orthogonality, we recover the local projection scheme with exception of the projection of $\nabla \cdot \mathbf{u}$.

$$\mathcal{S}_{lps}(U,V) \;=\; (\bar{\varkappa}_h \nabla p, \delta^p \bar{\varkappa}_h \nabla q) \;+\; (\bar{\varkappa}_h \nabla \mathbf{u}, \delta^u \bar{\varkappa}_h \nabla \mathbf{v})\,.$$

(ii) *Projection-based stabilization using inf-sup stable velocity-pressure pairs:*

In the case of inf-sup stable velocity-pressure pairs with $\mathbf{W}_h^{r,s} = \mathbf{V}_h^r \times \mathbf{Q}_h^s$, a pressure stabilization is not necessary, hence we consider

$$\mathbf{G}_{H,U} = \mathbf{G}_H \times (\nabla \mathbf{Q}_h^s). \tag{75}$$

where $\mathbf{G}_H$ denotes a finite dimensional space of $d \times d$ tensors. Moreover, let $\delta(U_h, h)$ denote an additional viscosity. The *coarse space projection based* method reads:
find $\{U_h, \mathbb{G}_H\} \in \mathbf{W}_h^{r,s} \times \mathbf{G}_H$ s.t.

$$\begin{aligned} \mathcal{A}(\mathbf{b}; U_h, V_h) + (\delta(U_h,h)(\nabla \mathbf{u}_h - \mathbb{G}_H), \nabla \mathbf{v}_h) &= \mathcal{L}(V_h) \quad \forall\, V_h \in \mathbf{W}_h^{r,s} \\ (\nabla \mathbf{u}_h - \mathbb{G}_H, \mathbb{L}_H) &= 0 \qquad \forall\, \mathbb{L}_H \in \mathbf{G}_H. \end{aligned} \tag{76}$$

A complete description requires the choice of the space $\mathbf{G}_H$ and of $\delta(U_h, h)$. For the numerical analysis, we refer to [24, 25].

### 5.4 Evaluation of symmetric stabilization methods

Striking *advantages* of symmetric stabilized methods are that a separation of velocity and pressure in the stabilization terms occurs and that the evaluation of second-order derivatives (of the velocities) is avoided. An important *disadvantage* is that the FE stencil is (much) less compact than for classical residual-based methods. As a consequence, the data structure is more involved, e.g., the efficient calculation of the (local) projections within the two-level approach.

A systematic comparison of the theoretical aspects of such methods is given in the review paper [5]. The numerical analysis of symmetric stabilized schemes is still in its infancy as compared to the classical residual-based methods. In particular, results for hybrid meshes with anisotropic layer refinement are open. Another important goal of future research is to provide a critical (but fair) practical comparison of different methods.

## 6 SUMMARY. CONCLUSIONS

In this review paper, we considered stabilization techniques for linearized Navier-Stokes flow (Oseen model) which appears as auxiliary problem in the calculation of nonstationary

incompressible flows. For classical residual-based methods, like the SUPG/PSPG scheme with grad-div stabilization, there exists now an almost convincing a-priori analysis which covers important aspects like robustness w.r.t. viscosity and time stepping, higher-order elements, and anisotropic mesh refinement in layers. Moreover, and as a surprising result, the PSPG terms can be omitted for inf-sup stable velocity-pressure FE pairs.

The picture is less complete for the a-posteriori analysis of the Oseen model (not considered here). For some important results on isotropic meshes, we refer to [3].

Some drawbacks of classical residual-based stabilization schemes stem from the strong coupling of velocities and pressure in the stabilization terms. As a remedy, symmetric stabilization schemes have been considered recently. Further research is necessary in order to circumvent some disadvantages of these new methods like the more complicated data structure.

## REFERENCES

[1] Th. Apel. *Anisotropic finite elements: Local estimates and applications.* Series "Advances in Numerical Mathematics", Teubner, Stuttgart, 1999.

[2] Th. Apel, T. Knopp and G. Lube. Stabilized finite element methods with anisotropic mesh refinement for the Oseen problem. submitted to *Appl. Num. Math. 2006*

[3] S. Berrone. Adaptive discretizations of differential models in fluid dynamics, Dipartimento di Ingegneria Aeronautica, Politecnico di Torino. Ph.D. Thesis 2000

[4] M. Braack and E. Burman. Local projection stabilization for the Oseen problem and its interpretation as a variational multiscale method. *SIAM J. Numer. Anal.* Vol. 43(6) (2006), pp. 2544-2566.

[5] M. Braack, E. Burman, V. John, G. Lube. Stabilized finite element methods for the generalized Oseen problem, NAM-Preprint 2005.30. to appear in Comp. Meth. Appl.Mech. Engrg.

[6] F. Brezzi, B. Cockburn, L.D. Marini and E. Süli. Stabilization mechanisms in discontinuous Galerkin finite element methods. Oxford Univ. Comput. Lab., Report no. NA-04/24.

[7] A.N. Brooks and T.J.R. Hughes. Streamline upwind Petrov-Galerkin formulation for convection dominated flows with particular emphasis on the incompressible Navier-Stokes equations. *Comput. Methods Appl. Mech. Engrg.* 32 (1982), 199-259.

[8] E. Burman, M.A. Fernández and P. Hansbo. Continuous interior penalty method for the Oseen's equations. To appear in *SIAM J. Numerical Analysis*, (2006).

[9] E. Burman and M. Fernández. Stabilized finite element schemes for incompressible flow using velocity/pressure spaces satisfying the LBB-condition. In Proceedings of the 6th World Congress in Computational Mechanics, WCCM VI, 2004.

[10] B. Cockburn, G. Kanschat and D. Schötzau. The local discontinuous Galerkin method for the Oseen equations. *Math. Comp.* 73 (2004) 569-583

[11] R. Codina and J. Blasco. A finite element formulation of the Stokes problem allowing equal velocity-pressure interpolation. *Comp. Meth. Appl. Mech. Engrg.* 143 (1997) 373-391.

[12] R. Codina. Stabilization of incompressibility and convection through orthogonal subscales in finite element methods. *Comp. Meth. Appl. Mech. Engrg.* 190 (13/14) (2000) 1579-1599.

[13] R. Codina, O. Soto. Approximation of the incompressible Navier-Stokes equations using orthogonal subscale stabilization and pressure segregation on anisotropic finite element meshes, *Comput. Meth. Appl. Mech. Engrg.* 193 (2004) 1403–1419.

[14] L.P. Franca and S.L. Frey. Stabilized finite element methods: II. The incompressible Navier-Stokes equations. *Comp. Meth. Appl. Mech. Engrg.* 99 (1992) 209-233.

[15] T. Gelhard, G. Lube, M.O. Olshanskii and J.H. Starcke. Stabilized finite element schemes with LBB-stable elements for incompressible flows. *J. Comp. Applied Math.* 177 (2005) 243-267.

[16] V. Girault, B. Riviere, and M.F. Wheeler. A discontinuous Galerkin method with nonoverlapping domain decomposition for the Stokes and Navier-Stokes problems. *Math. Comp.* 74 (2004) 249, 53-84.

[17] J.-L. Guermond. Stabilization of Galerkin approximations of transport equations by subgrid modeling. *M2AN*, 33 (1999) 1293-1316.

[18] P. Hansbo and A. Szepessy. A velocity-pressure streamline diffusion finite element method for the incompressible Navier-Stokes equations. *Comput. Meths. Appl. Mech. Engrg.* 84 (1990) 175-192.

[19] P. Houston and E. Süli. Stabilised hp-finite element approximations of partial differential equations with nonnegative characteristic form. *Computing* 66 (2001), 99-119

[20] T.J.R. Hughes. Multiscale phenomena: Green's functions, the Dirichlet-to-Neumann formulation, subgrid-scale models, bubbles and the origin of stabilized methods. *Comp. Meth. Appl. Mech. Engrg.*, 127 (1995) 387-401.

[21] T.J.R. Hughes, L.P. Franca and M. Balestra. A new finite element formulation for computational fluid dynamics: V. Circumventing the Babuska-Brezzi condition: A stable Petrov-Galerkin formulation of the Stokes problem accomodating equal-order interpolations. *Comput. Meths. Appl. Mech. Engrg.* 59 (1986), 85-99.

[22] T.J. Hughes, L. Mazzei, and K.E. Jansen. Large eddy simulation and the variational multiscale method. *Comput. Visual. Sci.*, 3 (2000) 47 – 59.

[23] V. John. Large Eddy Simulation of Turbulent Incompressible Flows. Analytical and Numerical Results for a Class of LES Models. *Lecture Notes in Computational Science and Engineering*. Vol. 34. Springer-Verlag 2004.

[24] V. John and S. Kaya. Finite element error analysis of a variational multiscale method for the Navier-Stokes equations. *Adv. Comp. Math.*, in press, 2006.

[25] V. John and S. Kaya. A finite element variational multiscale method for the Navier-Stokes equations. *SIAM J. Sci. Comp.*, 26 (2005) 1485 – 1503.

[26] C. Johnson and J. Saranen. Streamline diffusion methods for the incompressible Euler and Navier-Stokes equations. *Math. Comp.* 47 (1986) 175, 1-18.

[27] S. Kaya and W.J. Layton. Subgrid-scale eddy viscosity models are variational multiscale methods. Technical Report TR-MATH 03-05, University of Pittsburgh, 2003.

[28] T. Knopp, G. Lube, R. Gritzki, M. Rösler. A near-wall strategy for buoyancy-affected turbulent flows using stabilized FEM with applications to indoor air flow simulation. *Comput. Meths. Appl. Mech. Engrg.* 194 (2005) 36-38, 3797-3816.

[29] G. Lube and G. Rapin. Residual-based stabilized higher-order FEM for a generalized Oseen problem. To appear in *Math. Model. Meths. Appl. Sc.* 2006

[30] G. Matthies. Private communication (2006)

[31] L. Tobiska and G. Lube. A modified streamline diffusion method for solving the stationary Navier-Stokes equations. *Numer. Math.* 59 (1991), 13-29.

[32] L. Tobiska and R. Verfürth. Analysis of a streamline-diffusion finite element method for the Stokes and Navier-Stokes equations. *SIAM Numer. Anal.* 33 (1996), 107-127.

Institut für Numerische und Angewandte Mathematik
Universität Göttingen
Lotzestr. 16-18
D - 37083 Göttingen

Telefon: 0551/394512
Telefax: 0551/393944

Email: trapp@math.uni-goettingen.de URL: http://www.num.math.uni-goettingen.de

## Verzeichnis der erschienenen Preprints:

| | | |
|---|---|---|
| 2006-01 | R. Schaback | Limit Problems for Interpolation by Analytic Radial Basis Function |
| 2006-02 | N. Bissantz, T. Hohage, A. Munk, F. Ruymgaart | Convergence rates of general regularization methods for statistical inverse problems and applications |
| 2006-03 | J. Brimberg, H. Juel, A. Schöbel | Locating a circle on a sphere |
| 2006-04 | J. Brimberg, H. Juel, A. Schöbel | Locating a circle on the plane using the minimax criterion |
| 2006-05 | L. Ling, R. Opfer, R. Schaback | Results on Meshless Collocation Techniques |
| 2006-06 | G. Lube, T. Knopp et.al. | Domain decomposition methods for indoor air flow simulation |
| 2006-07 | T. Apel, T. Knopp, G. Lube | Stabilized finite element methods with anisotropic mesh refinement for the Oseen problem |
| 2006-08 | R. Schaback | Recovery of Functions From Weak Data Using Unsymmetric Meshless Kernel-Based Methods |
| 2006-09 | H.W. Hannacher, S. Horn, A. Schbel | Stop Location Design in Public Transportation Networks: Covering and Accessibility Objective |
| 2006-10 | Q.T. Le Gia, F.J. Narcowich, J.D. Ward, H. Wendland | Continuous and Discrete Least-Squares Approximation by Radial Basis Functions on Spheres |
| 2006-11 | R. Schaback | Unsymmetric Meshless Methods for Operator Equations |

| | | |
|---|---|---|
| 2006-12 | P. Giesl, H. Wendland | Meshless Collocation: Error Estimates with Application to Dynamical Systems |
| 2006-13 | H. Wendland | On the stability of meshless symmetric collocation for boundary value problems |
| 2006-14 | G. Lube | Stabilized FEM for incompressible flow. Critical review and new trends |